Journal of Photochemistry & Photobiology, B: Biology 205 (2020) 111846

Contents lists available at ScienceDirect

Journal of Photochemistry & Photobiology, B: Biology

journal homepage: www.elsevier.com/locate/jphotobiol

Phytosomal nanocarriers as platforms for improved delivery of natural antioxidant and photoprotective compounds in propolis: An approach for enhanced both dissolution behaviour in biorelevant media and skin retention profiles

Andi Dian Permana[a,b,*], Rifka Nurul Utami[c], Aaron J. Courtenay[a], Marianti A. Manggau[d], Ryan F. Donnelly[a], Latifah Rahman[b,**]

[a] School of Pharmacy, Queen's University Belfast, Medical Biology Centre, 97 Lisburn Road, Belfast BT9 7BL, UK
[b] Department of Pharmaceutics, Faculty of Pharmacy, Hasanuddin University, Makassar, Indonesia
[c] College of Pharmacy STIFA Kebangsaan, Makassar, Indonesia
[d] Department of Pharmacology and Toxicology, Faculty of Pharmacy, Hasanuddin University, Makassar, Indonesia

ARTICLE INFO

Keywords:
Propolis
Phytosome
Natural antioxidant
Photoprotective
Dissolution enhancement
Antiaging

ABSTRACT

Propolis has been reported to possess rich content of antioxidant compounds and may provide health benefits through oxidative stress reduction. Presently, the formulation activities used to enhance the drug delivery have been hampered due to inherently low aqueous solubility and poor transdermal permeation of the bioactive phenols and flavonoids. Here, we show, the formulation of propolis extract (PE) into phytosome delivery systems. The optimum antioxidant activity was attained through extraction process using 75% *v*/v ethanol. The phytosome was prepared using thin-layer hydration technique with L-α-Phosphatidylcholine as a phospholipid. Fourier transform infrared (FTIR) was used to investigate the occurrence of molecular interactions between formulation components. This innovative approach could encapsulate > 40% of bioactive compounds in PE, namely caffeic acid, quercetin, and kaempferol. FTIR spectroscopy indicated new hydrogen bond formation, supporting successful phytosome formulation. The phytosomes enhanced the dissolution up to 4-folds of bioactive compounds in bio-mimicked release media, as well as improved penetrability and skin retention up to 6-folds of the three main compounds of propolis, when compared to non-encapsulated PE formulation. Importantly, the hydrogel containing phytosome showed a potential for UVA and UVB radiation absorption, indicated by the SPF values of higher than 15. To conclude, this work shows promising novel delivery approaches for PE in the treatment of organ injured stress oxidative and skin aging.

1. Introduction

Free radicals, including reactive oxygen species (ROS) and reactive nitrogen species (RNS), have a considerable impact on human health. Due to their reactivity, free radicals are able to interact with biological molecules, such as lipids, proteins and DNA, causing damage that may eventually lead to cell death. The imbalance of free radicals and body antioxidants leads to a condition called oxidative stress [1,2]. An extensive number of studies has established the link between oxidative stress and various medical conditions. Firstly, researchers have found correlations between oxidative stress and the aetiology of numerous diseases. The group of diseases includes, but is not limited to, cardiovascular diseases [3], autoimmune diseases [4,5], neurodegenerative diseases [6], chronic kidney disease [7], liver diseases [8] and cancer [9]. Secondly, oxidative stress has been found to be the primary causes of skin aging. Some biochemical responses within the human body, as well external factors, produce ROS [10]. The production of ROS in the skin is initiated by UV radiation which leads to lipid peroxidation in cells, resulting in mitochondrial damage [11]. These radicals decrease the collagen and elastin in the skin. This will consequently cause thinning, loosening, and wrinkling of the skin. These findings have brought the important

* Corresponding author at: School of Pharmacy, Queen's University Belfast, Medical Biology Centre, 97 Lisburn Road, Belfast BT9 7BL, UK; Faculty of Pharmacy, Hasanuddin University, Indonesia
** Corresponding author.
E-mail addresses: apermana01@qub.ac.uk (A.D. Permana), tifah_rahman15@yahoo.com (L. Rahman).

https://doi.org/10.1016/j.jphotobiol.2020.111846
Received 14 December 2019; Received in revised form 18 February 2020; Accepted 2 March 2020
Available online 02 March 2020
1011-1344/

role of antioxidants into perspective. Although synthetic antioxidants have been widely investigated, the natural sources continue to be the leading reservoir of antioxidant compounds. To date, extensive numbers of studies have been carried out on natural sources, particularly on those containing polyphenols and flavonoids which have been proven to exhibit antioxidant activities [12,13]. Compared to their synthetic counterparts, natural antioxidants possess several advantages, including fewer side effects and lower financial costs. Therefore, there is a need to develop novel antioxidant compounds from natural sources.

Propolis, a bee product, is one example of a natural product with promising antioxidant activity. Propolis is often referred to as "bee glue" and is described as a resinous material produced by honeybees from leaves, flowers, sprouts, or other parts of various plants [14]. The excellent antioxidant activity of propolis has been attributed to the high content of flavonoid and other phenolic compounds [15]. Additionally, caffeic acid (CA), quercetin (QU) and kaempferol (KP) contained in propolis have all shown strong antioxidant capacity to protect body tissues from oxidative stress [16–19]. These three compounds have also been reported to have anti-aging properties. However, significant problem arises because of the nature of these compounds. They have all been reported to exhibit low solubility, poor dissolution profiles and reduced skin permeation abilities [18–21]. This will consequently hinder the permeability of the substances through biological membranes. Thus, the development of suitable delivery systems to help increase the permeability of these natural substances is necessary to achieve optimum therapeutic efficacy.

Phytosomes are a type of vesicular nanocarrier delivery system having similar structure to liposomes, where the encapsulated phytoconstituents form a molecular level complexation *via* hydrogen bonds with the phospholipids [22]. Phytosomes are prepared using various types of solvent. Generally, polar aprotic solvents are typically used in phytosome preparation to provide a suitable environment supporting hydrogen bond formation [22–24]. However, these solvents have been replaced by the utilisation of protonic solvent, such as ethanol and methanol [25–27]. Indeed, the formation of hydrogen bonding has also been reported in methanol [28,29]. The formation of hydrogen bonds between the entrapped compounds and the phospholipid offers several benefits, namely high entrapment efficiency, better stability profile and increased permeability through biological membranes, therefore resulting in enhanced bioavailability and greater efficacy [22,23,30,31]. Several studies have shown the successful formulation of some phytoconstituents into phytosome, for instance apigenin [23], *Centella asiatica* extract [32], *Vitis vinifera* L. seed extract [33] showing that the formulation of these natural products into phytosomes exhibited greater dissolution, stability, bioavailability profiles and dermal retention profiles. Taking a lead from these previous promising studies, the formulation of propolis extract (PE) loaded into phytosome delivery system could provide a promising system to enhance the stability and release profiles of the bioactive compounds from propolis into biological fluid.

In the present study, we outline the innovative formulation of PE-loaded phytosomes (PEP) using phosphatidylcholine. Initially, in order to achieve the maximum phenolic and flavonoid content, the extraction solvent selection was optimised, the total phenolic content (TPC) and total flavonoid content (TFC) determined, antioxidant activity and sun protective factor (SPF) value were investigated. Following this, we formulated, optimised and characterised the PEP, and carried out solubility studies of the PEP. Finally, taking into consideration that antioxidants can be beneficial for human health in many aspects, for the first time, we studied the release profiles PEP in two different methods, namely dissolution study in biorelevant media, as well as skin permeation and retention studies in rat's skin. The biorelevant media was used to represent the condition of gastrointestinal tract, while rat's skin was used to evaluate the dermal delivery of this approach.

2. Materials and Methods

2.1. Materials

Propolis from *Apis mellifera* was obtained from Forestry Faculty, Hasanuddin University, Indonesia. Ethanol was purchased from Merck, Darmstadt, Germany. 2, 2-diphenyl-1-picrylhydrazyl (DPPH), acetonitrile for HPLC, caffeic acid, kaempferol, L-α-Phosphatidylcholine (PC) from egg yolk and quercetin were purchased from Sigma–Aldrich Pte Ltd., Singapore, Singapore. All other reagents used were analytical grade.

2.2. Methods

2.2.1. Optimisation of Propolis Extraction Method

Raw propolis (500 g) was extracted using 1 L of ethanol in water at varied concentration (25%, 50%, 75% and 100% *v*/v in water). The extraction process was carried out for 24 h in an ultrasonic bath (Bandelin Sonorex Digitec, Germany) at room temperature. Afterwards, the mixtures were filtered and then kept at 4 °C for 24 h. In an attempt to remove the wax, the mixtures were filtered again. The propolis extract (PE) obtained from 100% *v*/v ethanol (E100) was dried directly using a rotary evaporator (Büchi Rotavapor R-114, Büchi, Switzerland), obtaining PE. This PE, obtained from 25% (E25), 50% (E50) and 75% ethanol (E75) was then subjected to a freeze drying (Movel Scientific Instrument Co., Zhejiang, China) to obtain dry extract. For water extract (WE), the dry extract was obtained by subjecting the extract directly to freeze drying.

2.2.2. Extraction Yields of Propolis

The extraction yield was calculated based on the mass of dried PE obtained by using the following equation:

$$\text{Extraction yield (\%)} = \frac{W\ dried\ extract}{W\ propolis} \text{ x } 100\% \quad (1)$$

where, *W dried extract* represents the weight of the dried PE and *W propolis* represents the initial weight of propolis.

2.2.3. Total Phenolic and Flavonoid Contents

Determination of the total phenolic content (TPC) of PE was carried out using the Folin-Ciocalteu method [34,35]. Initially, the dried PE was dissolved in methanol, resulting in a concentration of 1 mg/mL. Following this, 250 μL of the solution was mixed with 5 mL of distilled water and 0.5 mL of 1 N Folin-Ciocalteu reagent. This mixture was incubated at room temperature for 5 min. After that, 0.5 mL of 5% *w/v* sodium carbonate solution was added. The volume was made up to 10 mL with methanol. The mixture was again incubated in dark for 30 min at room temperature, and then homogenised. Absorbance of the mixture was measured at a wavelength of 760 nm using a spectrophotometer (Model UV-2500, Shimadzu Co., Ltd., Tokyo, Japan). TPC of PE was calculated from gallic acid standard curve. Results were expressed as milligrams of gallic acid equivalent per gram of propolis (mg GAE/g).

Determination of the total flavonoids content (TFC) was carried out with colorimetry using $AlCl_3$ [36,37]. Firstly, the dried PE was again dissolved in methanol, producing a concentration of 1 mg/mL and 0.5 mL of this solution was mixed with 0.25 mL of 10% *w/v* $AlCl_3$, 0.25 mL of potassium acetate. Samples were homogenised and left in the dark for 30 min. Finally, the absorbance was measured at 415 nm using a spectrophotometer (Model UV-2500, Shimadzu Co., Ltd., Tokyo, Japan). TFC was calculated from the calibration curve of quercetin. Results were expressed as milligrams of quercetin equivalent per gram of propolis (mg Qu/g).

2.2.4. Antioxidant Activity Assay Using DPPH Scavenging Capacity

2,2-diphenyl-1-picrylhydrozyl (DPPH) radical was used to

determine the antioxidant activity based on the free radical scavenging activities of the of PE [36,38]. In brief, 2.5 mL of DPPH solution in methanol (25 μg/mL) was mixed with 0.25 mL of various concentrations of PE solution in methanol (0.1–1.0 mg/mL) and 2.25 mL of methanol. Afterwards, the samples were incubated in the dark for 20 min at room temperature. Absorbance of the solution was then determined at 517 nm (Model UV-2500, Shimadzu Co., Ltd., Tokyo, Japan). As a control, the absorbance of the DPPH radicals without extract was also measured, and corresponding extraction solvents were used as blank. The absorbance of the samples was compared with those of the blank control. The determination was carried out in three replicates and averaged. Antioxidant activity was calculated as follows:

$$\%\text{Inhibition} = \frac{Abs\ control - Abs\ extract}{Abs\ extract} \text{ x } 100\% \quad (2)$$

Where *Abs control* represents absorbance of the control sample and *Abs extract* represents absorbance of the extract. Results were expressed as inhibition percentage. The concentration required to achieve a 50% inhibition of DPPH free radical (IC_{50}) was calculated using linear regression analysis in GraphPad Prism® version 6 (GraphPad Software, San Diego, California, USA).

2.2.5. Antioxidant Activity Using Lipid Peroxidation Method

Thiocyanate was used to determine the antioxidant activity of the PE. Briefly, linoleic acid emulsion was prepared by mixing 0.25 g of linoleic acid, 0.25 g of Tween-80 and 50 mL of 20 mM phosphate buffer pH 7.0 using an Ultra-Turrax® homogeniser (IKA, model T25, impeller 10 G, Germany). Different sample concentrations of PE were prepared in methanol. Afterwards, 0.5 mL of PE solution was mixed with 2.5 mL of linoleic acid emulsion and was incubated for 6 h at 37 °C. Aliquots (0.1 mL) were taken and were mixed with 5 mL of 75% ethanol, 0.1 mL of 30% *w/v* ammonium thiocyanate and 0.1 mL of 20 mM of ferrous chloride in 100 mM HCl. min. The absorbance of the linoleic acid emulsion without PE and PEP was used as the control for peroxidation. This mixture was incubated for 5 min at room temperature and the absorbance was determined at 500 nm. The percentage of lipid peroxidation inhibition was finally calculated using the following equation:

$$\text{Inhibition} = 100 - \left[\left(\frac{Abs\ extract}{Abs\ control}\right)x100\right] \quad (3)$$

where *Abs control* denotes absorbance of the control sample and *Abs extract* denotes absorbance of the extract. Results were presented as percentage of inhibition. The concentration required to achieve a 50% inhibition lipid peroxidation (IC_{50}) was calculated using linear regression analysis.

2.2.6. HPLC Assay of Bioactive Compounds in PE

The HPLC analysis of PE was carried out using reverse phase (Shimadzu Prominence, Shimadzu, Kyoto, Japan) system with LC-20AT quaternary gradient pump and Shimadzu LC solution software (ver. 1.21 SP1). The separation was performed using a reversed-phase column Gemini C18 (150 × 4.6 mm, 5 μm) (Phenomenex, Inc., CA, USA). A combination of 0.5% *v*/v acetic acid in water (A) and acetonitrile (B) was used as the mobile phase and a gradient condition over 30 min was applied to separate the compounds, as summarised in Table 1. The injection volume was 25 μL and the analyses were carried out at 40 °C with UV detection at 290 nm. As analytes of interest, concentrations of caffeic acid (CA), quercetin (QU) and kaempferol (KP) were measured in PE. The analytical methods were validated as per the International Committee of Harmonization (ICH) 2005 [39] and the validation results are shown in Tables S1 and S2.

Table 1
Gradient conditions for HPLC mobile phase.

Time	A (%)	B (%)	Flow (mL/min)
0	90	10	0.5
5	65	35	0.6
10	40	60	0.5
15	20	80	0.5
20	80	20	0.5
30	90	10	0.5

2.2.7. Phytosome Formulation

Propolis extract-loaded phytosome (PEP) was prepared using the thin-film hydration technique and solvent evaporation, as described previously, with slight modifications [23,30]. The compositions of each formulation investigated are summarised in Table 2. Cholesterol (0.5 g) was used in the same amount in all formulations. Briefly, PE, PC and cholesterol were dissolved in methanol for 60 min at 200 rpm. The solution was placed in a round bottom flask and was subjected to a vacuum rotary evaporator for 60 min at 55 °C and 50 rpm to remove the organic solvent. For the oral formulations, the resultant thin layer in the bottom flask was hydrated with 10 mL of distilled water, obtaining a PEP dispersion. Different particle size reduction methods were carried out, namely homogenisation at 10,000 rpm for 10 min, homogenisation at 10,000 rpm for 20 min, bath sonication 30 min and bath sonication for 60 min. For the oral delivery phytosome formulations, maltodextrin (5% *w/v*) was added to the dispersions prior to lyophilisation to obtain dry phytosome components.

2.2.8. Phytosome characterisation

2.2.8.1. Particle Size, PDI and Zeta Potential. The determination of particle size, PDI and zeta potential of the PEP vesicles were carried out using a Zetasizer (Malvern Zeta Sizer, Malvern Instruments, Malvern, UK), at 25 °C and a scattering angle of 90°. The PEP was diluted with distilled water prior to analysis.

2.2.8.2. Encapsulation Efficiency. The determination of encapsulation efficiency (EE) of compounds of interest (CA, QU and KP) was carried out by indirect technique. Briefly, the PEP dispersion was centrifuged for 60 min at 4 °C at 14,800 ×*g*. The concentration of un-encapsulated compounds present in the supernatant were quantified using the HPLC method described previously. Finally, the EE of the compounds was calculated using the following equation:

$$\text{EE}\ (\%) = \frac{a - b}{a}\ x\ 100\% \quad (4)$$

where *a* is the amount of compound added to the formulations and *b* is the amount of un-encapsulated drug.

2.2.8.3. Scanning Electron Microscope. The morphologies of PEPs were observed using a scanning electron microscope (SEM) (JEM-1400Plus; JEOL, Tokyo, Japan).

2.2.8.4. FTIR Study. The investigation of potential interactions between the compounds in PE and PC in PEP formulation was carried out using an FTIR spectrophotometer (Shimadzu® FTIR-8400). Briefly, PE, PC, and PEP were placed into the FTIR spectrophotometer and scanned over the 4000–600 cm^{-1} wavenumber region.

2.2.8.5. Solubility Analysis. The solubilities of CA, QU, and KP in PE after PEP preparation compared to crude extract were determined using a previously described method [23]. In brief, PE and PEP in excess were added into 15 mL of distilled water or n-octanol in sealed glass vials at ambient temperature. The mixture was then stirred for 1 h at 500 rpm, and centrifuged at 2.800 ×*g* for 15 min. The supernatant was collected and subjected to HPLC for analysis after suitable dilution.

2.2.9. In vitro Dissolution Study for Oral Delivery

The *in vitro* dissolution studies of PE and PEP were performed using USP dissolution apparatus II in 900 mL different release media, namely

Table 2
Details of the various formulation parameters used to prepare PEP and their respective particle size, PDI and zeta potential (means ± SD, n = 3).

Formulation code	E75	PC	Homogenisation	Bath sonication	Particle size (nm)	PDI	Zeta potential (mV)
F1	1 g	1 g	10 min	–	620 ± 54	0.234 ± 0.02	−31.44 ± 2.74
F2	1 g	1 g	20 min	–	532 ± 46	0.229 ± 0.02	−31.98 ± 2.78
F3	1 g	2 g	10 min	–	365 ± 32	0.244 ± 0.02	−34.09 ± 2.96
F4	1 g	2 g	20 min	–	336 ± 29	0.232 ± 0.02	−35.01 ± 3.04
F5	1 g	3 g	10 min	–	474 ± 41	0.265 ± 0.02	−37.41 ± 3.25
F6	1 g	3 g	20 min	–	448 ± 39	0.262 ± 0.02	−36.91 ± 3.21
F7	1 g	1 g	–	30 min	565 ± 49	0.261 ± 0.02	−30.98 ± 2.69
F8	1 g	1 g	–	60 min	321 ± 28	0.231 ± 0.02	−31.04 ± 2.70
F9	1 g	2 g	–	30 min	281 ± 24	0.253 ± 0.02	−32.45 ± 2.82
F10	1 g	2 g	–	60 min	248 ± 22	0.249 ± 0.02	−33.76 ± 2.93
F11	1 g	3 g	–	30 min	399 ± 35	0.243 ± 0.02	−34.32 ± 2.98
F12	1 g	3 g	–	60 min	368 ± 32	0.221 ± 0.01	−35.87 ± 3.12

fasted simulated small intestinal fluids (FaSSIF), fed state simulated small intestinal fluids (FeSSIF), and fasted state simulated gastric fluids (FaSSGF). FaSSIF (pH 6.5) was prepared from 0.42 g of NaOH, 3.0 mM of sodium taurocholate, 0,75 mM of PC, 4.47 g of Na_2HPO_4 and 6.169 g of NaCl in 1 L of water. FeSSIF (pH 5.0) was prepared from 4.04 g NaOH, 15 mM of sodium taurocholate, 3,75 mM of PC, 8.65 g of acetic acid and 11.87 g of NaCl in 1 L of water. FaSSGF (pH 1.5) was prepared from 1.999 g of NaCl and was adjusted to pH 1.5 with HCl 1 M. The dissolution was performed at 37 °C and 100 rpm. PE (100 mg) and an accurate amount of sample corresponding to 100 mg of PE were added into the dissolution media with 5 mL samples taken at predetermined time intervals and replaced with an equal volume of fresh release medium. To determine the amount of drug released from PEP, the samples were then analysed using HPLC after appropriate dilutions.

2.2.10. Drug Release Kinetic Using Mathematical Modelling

Different mathematic models were applied to the percentage of drug released as follows [40,41]:

$$\text{Zero order: } Q_t = Q_0 + K_0 t \quad (5)$$

$$\text{First order: } ln\, Q_t = ln\, Q_0 + K_1 t \quad (6)$$

$$\text{Higuchi: } Q_t = K_H \sqrt{t} \quad (7)$$

$$\text{Korsmeyer} - \text{Peppas: } Q_t = K_t n \quad (8)$$

$$\text{Hixson} - \text{Crowell: } Q_0^{1/3} - Q_t^{1/3} = K_s t \quad (9)$$

where Q_t (%) is the percentage of drug released at time t, Q_0 is the initial value of Q_t, t is the time, n is the diffusion release exponent, K_0, K_1, K_H, K_t and K_s are the release coefficients corresponding to relevant kinetic models. DDSolver was utilised to calculate the model parameters [42].

2.2.11. In vitro Phytosomal Stability in Gastrointestinal Environment

The selected PEP formulation was evaluated in terms of *in vitro* stability in FaSSGF, FaSSIF and FeSSIF release media. The PEP formulation was added into 10 mL of FaSSGF, FaSSIF, FeSSIF and PBS pH 7.4 and the samples were incubated at 37 °C for 1 h and 3 h. The particle size, PDI and zeta potential of each samples were evaluated as described previously (Method 2.2.8.a).

2.2.12. Preparation of Phytosomal Hydrogel for Dermal Delivery

Hydrogels were prepared by initially mixing Carbomer 940 (1.5% *w*/w) and glycerol (10% w/w) in distilled water and storing overnight at ambient temperature. Afterwards, 0.5% w/w of triethanolamine was added into the mixture, resulting in a clear hydrogel. Following the evaporation of organic solvent in PEP preparation, 5 mL of distilled water was added to hydrate the pyhtosome. The hydrated PEP was incorporated into the hydrogel with a ratio 1:9 (PEP:hydrogel). Hydrogel containing PE was prepared as a control.

2.2.13. Characterisation of Phytosomal Hydrogel

2.2.13.1. Drug Uniformity Content and pH. Drug uniformity was evaluated by collecting 0.5 g of PEP hydrogel from three independent sections of the container. The hydrogel was mixed with 5 mL of methanol and vortexed for 1 h. The dispersion was centrifuged at 4800 ×*g* for 15 min. The supernatant was collected and analysed for drug content using HPLC. pH of the hydrogel formulation was determined using pH meter.

2.2.13.2. Spreadability. A mass of hydrogel (500 mg) was placed on a glass plate and the diameter recorded. Another glass plate with a 500 g mass was placed on the top of the formulation. This was allowed to stand for 5 min and the diameter of hydrogel after spreading was recorded.

2.2.13.3. In Vitro Skin Occlusivity Evaluation. In vitro skin occlusivity was carried out using a previously described method [43]. A mass of 250 mg of formulation was applied to Whatman filter paper (cut off size 2.5 µm). The filter paper was used to cover a 100 mL beaker filled with 50 mL of distilled water. As control, a filter paper without formulation was used. The beakers were kept at 32 °C and the weight of the system was determined at 0 h, 6 h, 24 h and 48 h. The occulisivity (F_0) was calculated using following equation:

$$F0 = \frac{W0 - W1}{W0} x\ 100 \quad (10)$$

where, *W0* is the water loss of the control and *W1* is the water loss of the formulation group.

2.2.14. Ex-vivo Skin Permeation and Retention Studies

Ex-vivo skin permeation studies were carried out on 25 mL Franz diffusion cell with diffusional area of 1 cm^2. Abdominal skin of Male Sprague-Dawley rats was shaved and equilibrated in PBS (pH 7.4) containing 1% *w/v* Tween 80 as a medium prior to the experiment. Tween 80 was added into medium to achieve the sink condition. The receptor compartment was filled with the medium and the skin was mounted between the receptor and donor compartment. The assembly was kept at 37 °C and stirred at 100 rpm. Aliquots of 0.5 g of each formulation were applied to the donor compartment and 0.5 mL of receptor media was taken at predetermined time intervals and replaced with the same volume of fresh medium. The samples were then analysed using HPLC to determine the amount of drug permeated from PEP.

Skin drug retention was determined after 24 h following the skin permeation study. The skin was removed and washed three times with distilled water to remove any excess formulations. The skin was cut into small pieces and the drugs retained were extracted with methanol in bath sonicator for 6 h. The samples were centrifuged at 2800 ×*g* for 15 min. The supernatant was collected and was subjected to HPLC for analysis.

2.2.15. Antioxidant Activity and Sun Protective Factor (SPF) of Optimised Formulation

The selected formulations were dissolved in methanol using a bath sonicator for 1 h. The antioxidant activity of selected PEP formulation was carried out using the method described previously for PE.

SPF values of hydrogels containing PE and PEP were calculated using the method developed by Mansur et al. [44]. Briefly, the formulations corresponding to PE with the range concentration from 0.1 mg/mL to 1 mg/mL were prepared in methanol. The readings of measurement were carried out from 200 nm to 400 nm wavelength to evaluate the absorption in the UVA (320–400 nm) and UVB (280–320 nm). The absorption of each solution was measured between 290 and 320 nm with intervals of 5 nm using a spectrophotometer (Model UV-2500, Shimadzu Co., Ltd., Tokyo, Japan). SPF values were calculated using the Eq. (11):

$$\mathrm{SPF} = CF \times \Sigma \frac{320\ nm}{290\ nm} EE_{\lambda} \times I_{\lambda} \times Abs_{\lambda} \quad (11)$$

where, *CF* is 10 (constant), EE is erythemogenic effect, I is intensity of the sun and Abs is absorbance of the samples.

2.2.16. Statistical Analysis

All data were expressed as means ± standard deviation (SD) of the mean. The calculation of SD was conducted using Microsoft® Excel® 2016 (Microsoft Corporation, Redmond, USA). Statistical analysis was performed using GraphPad Prism® version 6 (GraphPad Software, San Diego, California, USA). Where appropriate, an unpaired *t*-test was carried out for comparison of two groups. The Kruskal-Wallis test with post-hoc Dunn's test was carried out for comparison of multiple groups. In all cases, $p < .05$ was represented as a significant difference.

3. Results and Discussion

3.1. Extraction Yield, TPC, and TFC of PE

Propolis has been reported to have excellent antioxidant activity due to its phenolic and flavonoid compounds [15]. Phenolic and flavonoid compounds of propolis can potentially act as protective agents to avoid oxidative damage caused by free radicals [45,46]. Accordingly, in this study, we initially investigated the effect of the extracting solvent on the extraction yield, TPC, TFC and antioxidant activity (expressed as IC_{50}) of PE. Fig. 1A–C present the extraction yield, TPC and TFC of PE. The results revealed that the higher the ethanol concentration, the higher the yield of PE. We showed the lowest extraction yield at 2.77 ± 0.04% *w*/w, while E100 exhibited 49.12 ± 1.54% w/w extraction yield. In terms of TPC and TFC values, PE obtained from E75 showed the greatest TPC and TFC, which were 179.32 ± 9.32 mg/g PE (equal to gallic acid) and 277.21 ± 3.43 mg/g PE (equal to quercetin), respectively. In addition, these values were significantly higher ($p < .05$) than the TPC and TFC obtained from E100, E50, E25 and WE. The results indicated that the combination of high ethanol, low water could extract a rich variety of phenolic and flavonoid compounds. Propolis contains a variety of phenolic and flavonoid compounds of varying polarity [47,48]. Therefore, the mixture of ethanol and water was able to extract numerous types of bioactive compounds.

3.2. Antioxidant Activity Assay Using DPPH Scavenging Capacity

Antioxidant activities of PE obtained from different solvents were also evaluated. The role of antioxidant is imperative in preventing numerous medical conditions caused by oxidative stress [1]. In this study, consistent with the TPC and TFC values of PE, E75 possessed the strongest antioxidant property against DPPD free radical compared to PE obtained from other solvents, indicated by the lowest IC_{50} value. This can be explained by the fact that two major phytochemical classes that can act as antioxidants are phenolic and flavonoid compounds [15]. As shown in Fig. 1F, the IC_{50} of PE against DPPH were 74.48 ± 4.32 μg/mL, 43.29 ± 3.02 μg/mL, 72.34 ± 5.09 μg/mL, 863.44 ± 65.4 μg/mL and 1454 ± 100.4 μg/mL for E100, E75, E50, E25 and WE, respectively.

3.3. Antioxidant Activity Using Lipid Peroxidation Method

The IC_{50} of PE against lipid peroxidation were 132.34 ± 10.12 μg/mL, 65.32 ± 3.43 μg/mL, 130.08 ± 12.33 μg/mL, 1503 ± 103.4 μg/mL and 2903.4 ± 200.4 μg/mL for E100, E75, E50, E25 and WE, respectively (Fig. 1I). The lipid peroxidation assay is important to determine the protective capability of antioxidant compounds in preventing cellular membrane damage caused by peroxyl radicals. The ability of antioxidants to prevent lipid peroxidation is based on the fact that lipids are the major biomolecules that compose cellular membrane.

3.4. HPLC Assay of Bioactive Compound in PE

This study was designed to understand the efficacy of phytosomes as nanoparticulate delivery systems containing PE through oral and dermal routes. Therefore, several compounds in PE obtained from different extraction solvents were also analysed. In this study, CA, QU and KP were selected as the compounds of most interest. Fig. 1J and K represent the HPLC chromatogram of CA, QU and KP in PE obtained from E75 and the concentration of these compounds in PE obtained from different solvents. The amounts of CA found in PE were 4.13 ± 0.02 mg/g, 4.15 ± 0.01 mg/g, 4.12 ± 0.03 mg/g, 2.87 ± 0.01 mg/g and 1.92 ± 0.01 mg/g for E100, E75, E50, E25 and WE, respectively. With respect to QU content, the amounts were found to be 0.73 ± 0.02 mg/g for E100, 0.72 ± 0.01 mg/g for E75 and 0.73 ± 0.03 mg/g for E50. However, due to the non-polar nature of QU, this compound was not found in E25 and WE. The concentration of KP found in PE were 2.66 ± 0.02 mg/g for E100, 2.62 ± 0.01 mg/g for E75, 2.63 ± 0.01 mg/g for E50, 0.48 ± 0.01 mg/g for E25 and 0.11 ± 0.01 mg/g for WE. The results revealed that the highest concentration of the three main compounds in PE were achieved using E75 as the extraction solvent. Bearing this in mind, combined with the results obtained in the TPC, TFC and antioxidant activity, PE extracted using E75 was finally selected for the further studies.

3.5. Phytosome Formulation

Several parameters were attempted in the optimisation of PEP formulation. Theoretically, phytosomes consist of a complex of phenolic and flavonoid with PC in 1:1, 1:2 or 1:3 M ratios [31,32,49,50]. However, due to the diversity of bioactive compounds in PE, the molar ratio was not used in this study. Instead, the weight ratio of PE and PC was used, which were 1:1, 1:2 and 1:3 weight ratios. Additionally, the effect of homogenisation and the sonication time were also evaluated. Fig. 3 presents the particle size, PDI, zeta potential as well as EE of CA, QU and KP in different PEP formulations.

As shown in Fig. 3, the high concentration of PC in PEP increased the particle size and PDI of phytosome. This may be caused by the increase of dispersion viscosity due to the increase of PC concentration, leading to the higher surface tension and hence larger particle size [51]. In addition, the increase of homogenisation and sonication time from 10 min to 20 min and from 30 min to 60 min, respectively, decreased the particle sizes significantly ($p < .05$). These processes were able to break down the vesicles into nano-size droplets. Moreover, prolonged homogenisation and sonication time produced more sonication energy to the nanoparticles dispersions, reducing the size of the phytosome droplets [52].

Regarding the zeta potential, the PE:PC ratio, homogenisation and sonication time did not exhibit a significant effect ($p > .05$) on the zeta potential of all PEP formulations. All formulations were found to

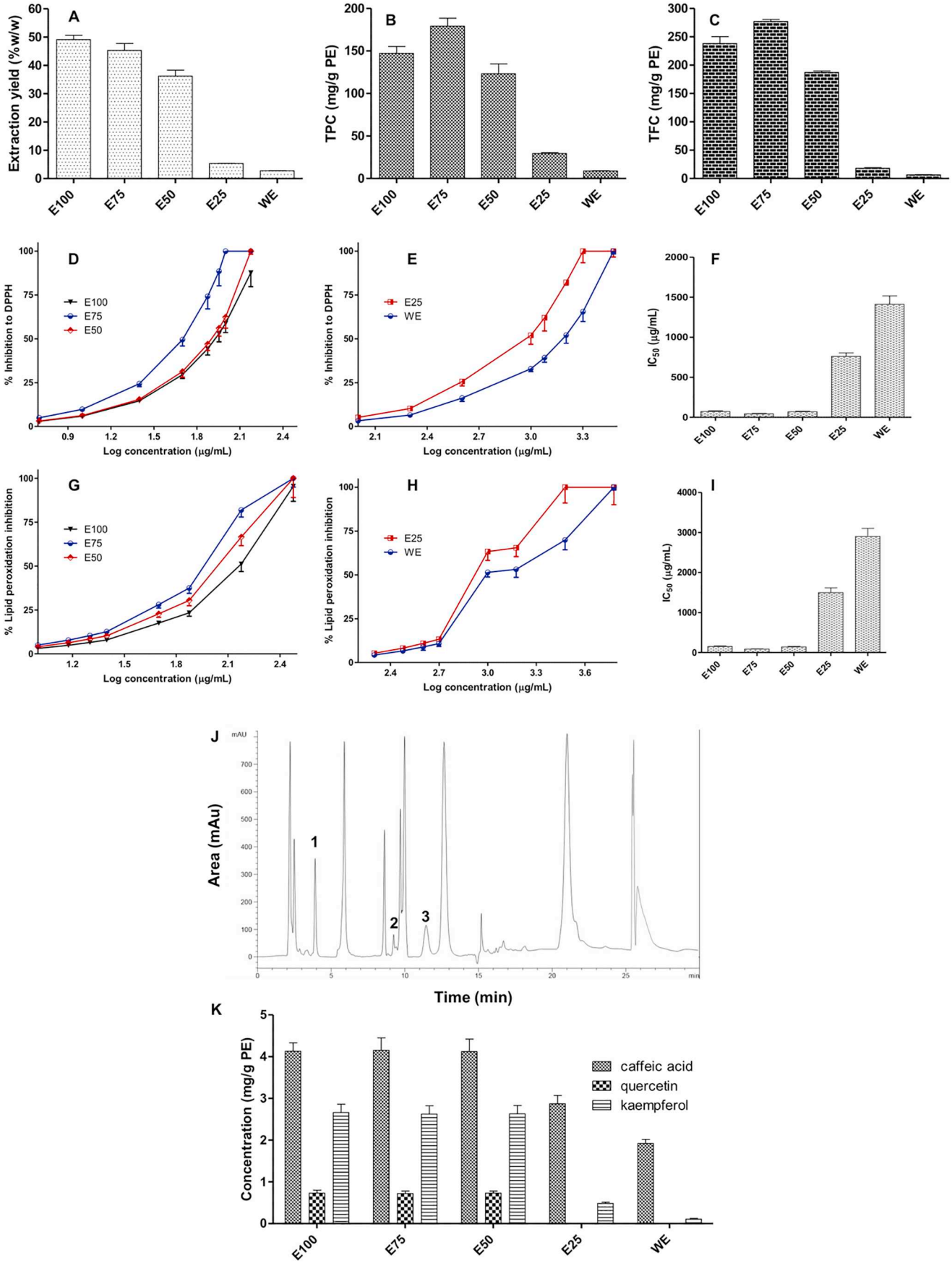

(caption on next page)

Fig. 1. The extraction yield (A), total phenolic content (B), total flavonoid content (C), the relationship between log concentration and inhibitory percentage against DPPH (D and E) and antioxidant activity (IC_{50}) (F) of PE extracted from different solvents, the relationship between log concentration and inhibitory percentage against DPPH (G and H) and antioxidant activity (IC_{50}) (I) of PE extracted from different solvents. HPLC chromatograms of chemical compounds in E75 at a wavelength of 280 nm (J), 1, 2 and 3 represents CA, QU, and KP, respectively. The concentration of CA, QU and KP calculated from PE extracted using different solvents (K) (means ± SD, n = 3).

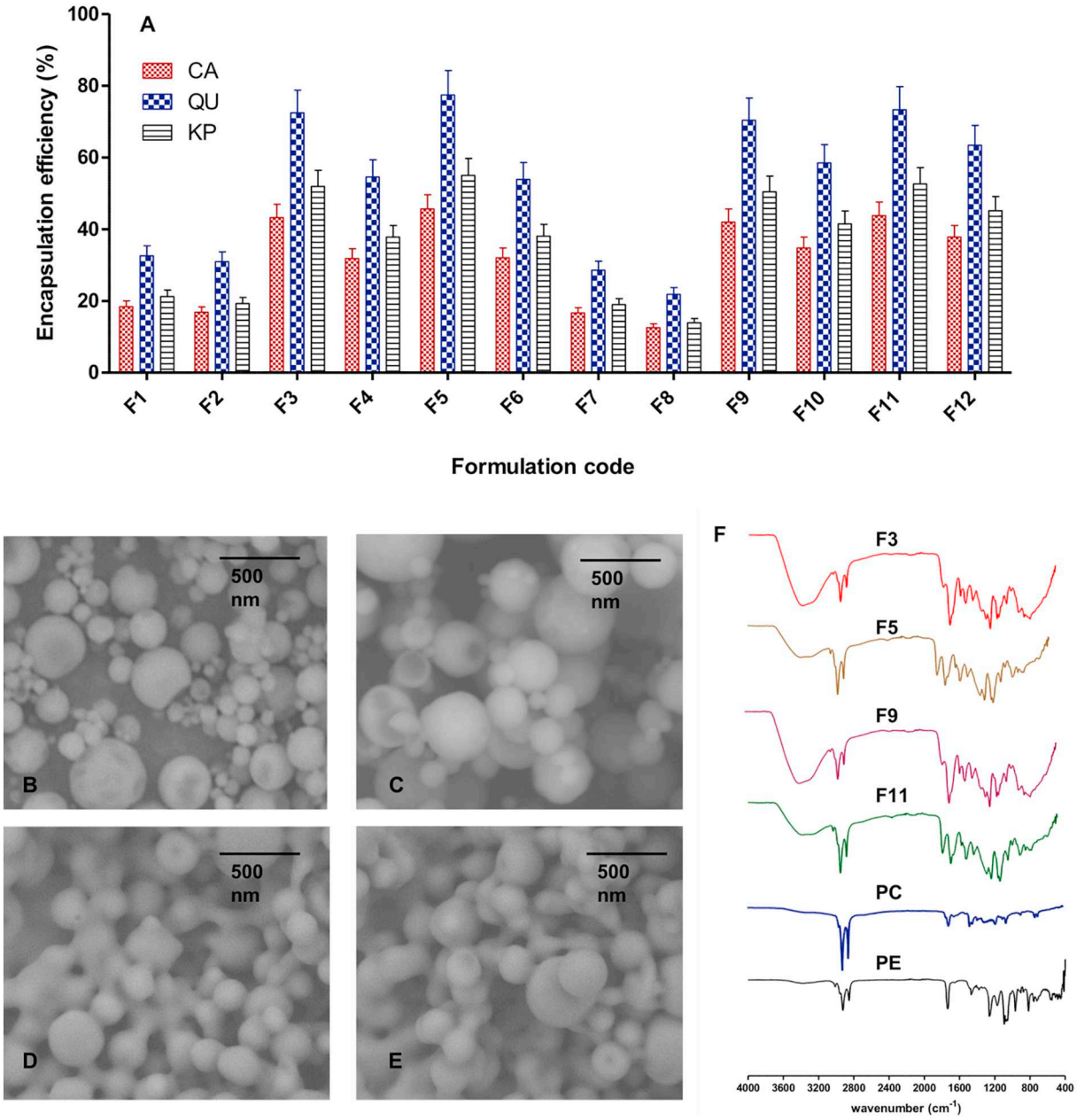

Fig. 2. Encapsulation efficiency of CA, QU and KP (A) of different PEP formulations (means ± SD, n = 3). SEM images of F3 (B), F5 (C), F9 (D) and F11 (E) formulation of PEP at a magnification power of 30,000×. FTIR spectra of F3, F5, F9 and F11 formulation of PEP, PC and PE (F).

have > −30 mV of zeta potential, indicating the excellent stability of PEP obtained in this study [53]. The negative zeta potential obtained in this study might be caused by the position of the negative phosphate group of PC which is toward to the outside layer of the phytosome [54].

With respect to the EE of PEP formulations, as described previously, the concentrations of CA, QU and KP encapsulated in PEP were determined. Fig. 2A depict the EE of CA, QU and KP in different PEP formulations. The results showed that these compounds had different capacity to be encapsulated in the PEP vesicles. The highest EE was achieved by QU, followed by KP and CA, respectively. This may be caused by the different of hydrogen donor and acceptor of these compounds. QU possesses 5 hydrogen bond donors and 7 hydrogen bond acceptors [55]. In contrast, CA and KP have 3 and 4 hydrogen bond donors as well as 4 and 6 hydrogen bond acceptors, respectively [56,57]. With this in mind, the possibility of QU to form hydrogen bond complex with PC was expected to be higher compared to those in CA and KP, resulting in higher EE in the PEP formulations. The EE of CA in PEP were in the range between 12.54 ± 1.09% and 45.65 ± 3.97%. The range of EE from 21.81 ± 1.89% to 77.44 ± 6.73% and from 13.90 ± 1.21% to 54.96 ± 4.78% in the case of QU and KP,

respectively. In the case of parameters observed, the higher EE of these compounds was achieved by using higher concentration of PC. Analysed statistically, the EE in PEP formulations prepared from 3 g of PC (F5, F6, F11 and F12) did not result in significantly higher EE compared to those prepared from 2 g of PC (F3, F4, F9 and F10) ($p > .05$). In addition, despite the decrease on the particle size, the utilisation of 20 min of homogenisation (F2, F4 and F6) and 60 min of sonication (F8, F10, and F12) resulted in significant reduction in the EE of all compounds in the PEP formulations ($p < .05$). This effect may be as a result of droplet break-up and separation of the core-shell formation of the composite nanoparticles, leading to increased leakage of the loaded drug throughout the emulsification process and therefore lower encapsulation efficiency [58]. Therefore, 10 min and 60 min were selected as an optimum time for homogenisation and sonication, respectively. Considering all these parameters, 4 formulations were selected for further studies, namely F3, F5, F9 and F11.

3.6. Scanning Electron Microscope and FITR Study

Fig. 2B–E depict the morphology of the phytosomal formulations observed by SEM. As shown, the obtained PEP exhibited spherical vesicles. The size of these phytosomes attained from SEM was in close agreement with the particle size results obtained from particle size analyser results.

FTIR studies were carried out on PE, PC and in the phytosomes to evaluate the existence of any interactions between bioactive compounds in PE and PC lipid. Fig. 2F shows the FTIR spectra of PE, PC and phytosome formulations. The FTIR spectrum of PC exhibited the characteristic signals at 2921 cm^{-1} and 2853 cm^{-1}, corresponding to the C—H stretching in the chain of long fatty acid. Additional signals were also observed at 1733 cm^{-1} (C═O stretching in the fatty acid ester), 1252 cm^{-1} (P═O stretching), 1093 cm^{-1} (P–O–C stretching), and 968 cm^{-1} [$-N^{+}(CH_2)^3$]. In the PE FTIR spectrum, the major peak was observed at 1694 cm^{-1} due to the C═O stretching of CA, QU and KP contained in PE. The peak at 1725 cm^{-1} was corresponding to carboxylic acid from *CA*. Due to the rich amount of phenolic compound in PE, the peak between 1200 and 1400 cm^{-1} were observed, corresponding to –OH phenolic bending. In PE formulation, it was found that the peaks of –OH and C═O of PE were shifted to a higher wave number. Furthermore, the peak of P═O of PC broadened. In addition, broadening of the characteristic phenolic (-OH) band at 3500 cm^{-1} was observed, which could be potentially caused by the formation of H-bonding [30].

3.7. Solubility Analysis

The effect of phytosome formulation on the apparent solubility of CA, QU and KP in PE was also investigated. The inherent solubilities of these compounds in water and n-octanol in comparison with their apparent solubilities in PEP formulations of F3, F5, F9 and F11 are depicted in Table 3. The inherent solubilities of CA, QU and KP in water were observed to be 143.23 ± 13.76 μg/mL 38.41 ± 2.54 μg/mL 37.34 ± 2.12 μg/mL, respectively. In n-octanol, these compound exhibited significant greater ($p < .05$) than those in water, which were 543.87 ± 49.12 μg/mL, 643.45 ± 19.88 μg/mL, and 654.32 ± 28.18 μg/mL for CA, QU and KP, respectively, representing the hydrophobic nature of these compounds. The formulation of PE into phytosome was able to enhance the apparent solubility of CA, QU and KP in both water and n-octanol. As shown in Table 3, in water, the solubilities of these compounds increased significantly ($p < .05$) over approximately 5-fold, 12-fold and 11-fold for CA, QU and KP, respectively, compared to their solubility in PE. The slight enhancements were observed in the solubility in n-octanol, which were approximately 1.1 times higher than those in the case of PE. Additionally, it was found that, despite the non-significant ($p > .05$) increase, the smaller particle size of PEP resulted in higher solubility in both water and n-octanol.

Table 3
Solubility of CA, QU and KP from pure PE and F3, F5, F9 and F11 of PEP formulations (means ± SD, n = 3).

Compound	Samples	Aqueous solubility (μg/mL)	n-octanol solubility (μg/mL)
CA	PE	143.23 ± 13.76	543.87 ± 49.12
	F3	832.12 ± 43.54	681.09 ± 52.10
	F5	759.36 ± 56.32	653.78 ± 48.77
	F9	895.43 ± 35.14	698.32 ± 32.12
	F11	787.13 ± 29.87	672.69 ± 29.13
QU	PE	38.41 ± 2.54	643.45 ± 19.88
	F3	471.12 ± 31.34	702.98 ± 35.31
	F5	398.95 ± 24.91	652.69 ± 30.87
	F9	483.23 ± 31.09	714.98 ± 31.32
	F11	426.98 ± 39.98	687.69 ± 38.15
KP	PE	37.34 ± 2.12	654.32 ± 28.18
	F3	371.02 ± 21.54	719.98 ± 32.87
	F5	345.87 ± 32.34	687.09 ± 41.93
	F9	398.45 ± 19.98	743.04 ± 53.16
	F11	378.98 ± 24.91	701.69 ± 49.23

Generally, phyto-phospholid complexes could potentially increase lipophilicty and hydrophilicty of active compounds [25]. Several studies have shown the ability of nanoparticle delivery system in enhancement the solubility of poorly water soluble drugs due to the reduction of the particle size [30,59,60].

3.8. In vitro Dissolution Study for Oral Delivery

In attempt to mimic human physiology, the *in vitro* dissolution behaviours of CA, QU & KP from PEP were investigated in three biorelevant media, namely FaSSGF, FaSSIF and FeSSIF. FaSSGH was used to stimulate condition in the stomach. While FaSSIF and FeSSIF were used to stimulated condition in the upper intestine [22,61–64]. The *in vitro* dissolution behaviours of CA, QU and KP in these media are depicted in Figs. 3, 4 and 5. In all cases, due to the hydrophobic nature of the compounds, the dissolution of CA, QU and KP from PE in all media was lower compared to those from PEP formulations.

Specifically, in FaSSGF, after 6-h, only 34.36 ± 1.9%, 29.52 ± 2.64% and 16.01 ± 1.44% of CA, QU and KP, respectively, were released in the case of PE, indicating low gastric dissolution of these compounds. Formulating PE into phytosome formulations was able to enhance the dissolution behaviour of these compounds in the gastric environment. As shown in Fig. 5, after 6-h 53.55 ± 4.91%, 37.87 ± 2.34%, 54.98 ± 2.44% and 38.65 ± 2.12% of CA were dissolved from F3, F5, F9 and F11, respectively. With respect to QU profile, the total dissolution of 49.72 ± 3.14%, 41.42 ± 3.87%, 55.67 ± 6.01% and 45.21 ± 3.10% were observed after 6-h dissolution of F3, F5, F9 and F11, respectively. In the case of KP profile, it was found that 45.65 ± 3.87%, 31.99 ± 2.10%, 52.98 ± 4.32% and 41.32 ± 4.01% of KP were dissolved from F3, F5, F9 and F11, respectively. With these results in mind, it was concluded that, despite the higher dissolution profile of PEP compared to PE, incomplete dissolution profiles in gastric environment were observed in all phytosome formulations. Accordingly, the dissolution behaviour in upper intestine is the key point for further dissolution profile of these compounds from PE and PEP.

In FaSSIF and FeSSIF, remarkably, CA, QU and KP experienced degradation due to the instability of these compound in the intestine environment. As illustrated in Fig. 5, in FaSSIF, CA, QU and KP were each degraded dramatically ($p < .05$) after 90 min, 75 min, 60 min, respectively. Rapid degradations to significant lower concentration ($p < .05$) of these compounds were observed in FeSSIF with time degradation of 75 min, 60 min and 45 min for CA, QU and KP, respectively. Incorporation of PE into phytosome formulation was shown to protect these compounds from the degradation in the intestine environment. After 6 h, 91.07 ± 8.20%, 63.98 ± 5.75% and

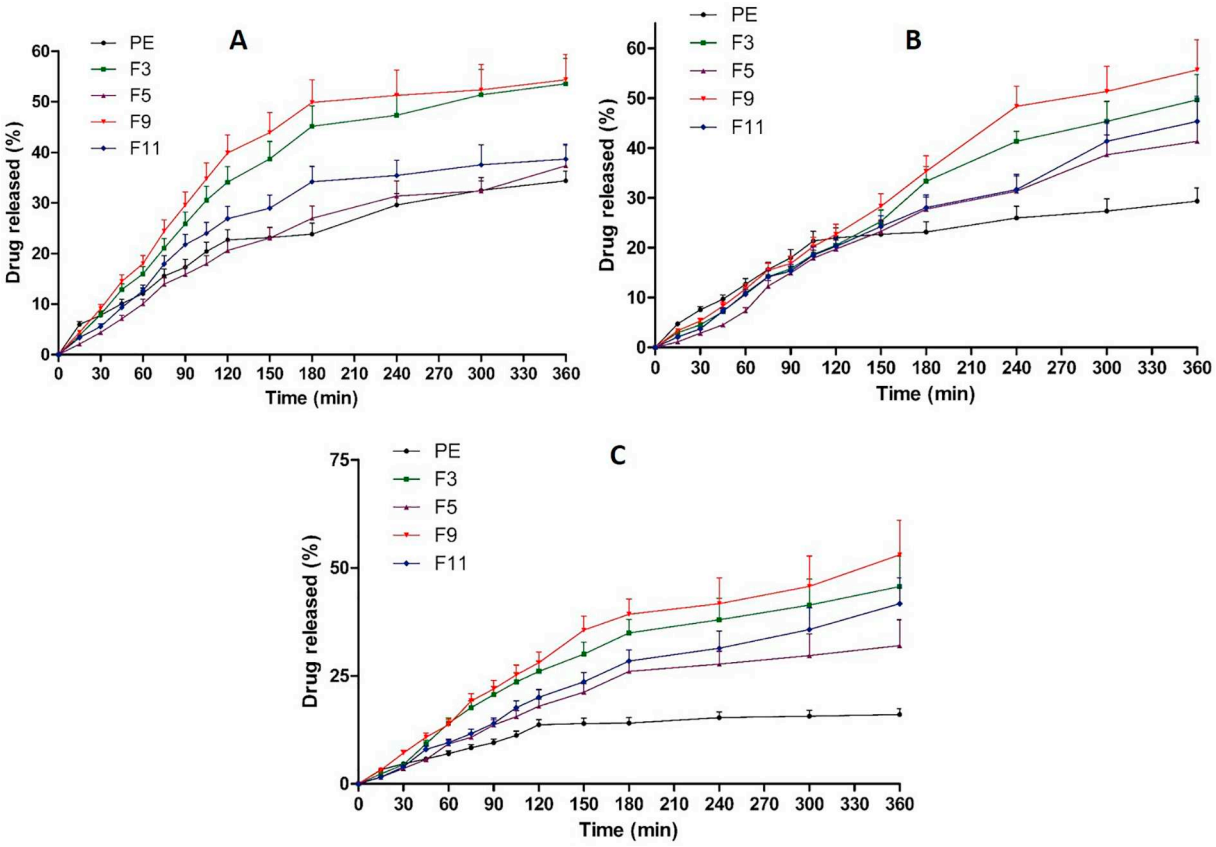

Fig. 3. *In vitro* dissolution profiles of CA (A), QU (B) and KP (C) in PE in comparison with different PEP formulations in FaSSGF, pH 1.6 at 37 ˚C (means ± SD, n = 3).

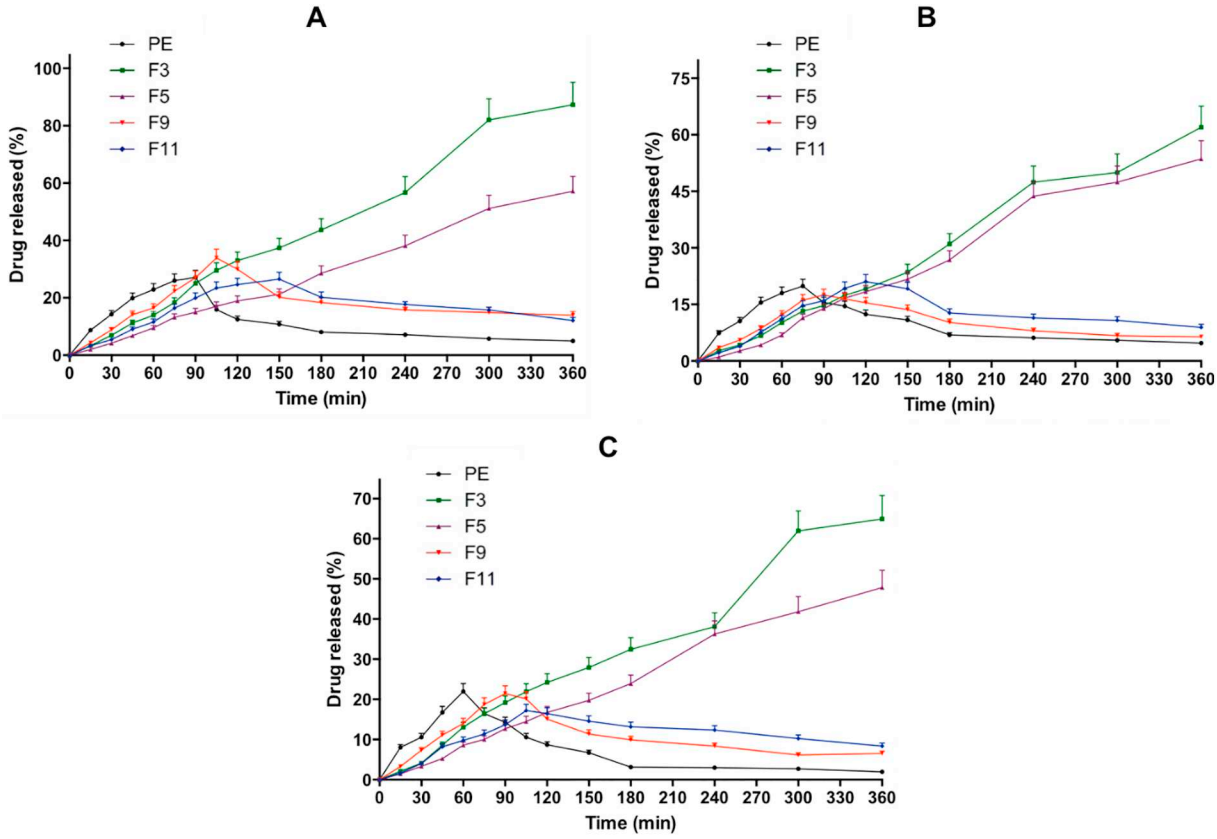

Fig. 4. *In vitro* dissolution profiles of CA (A), QU (B) and KP (C) in PE in comparison with different PEP formulations in FeSSIF, pH 5.0 at 37 ˚C (means ± SD, n = 3).

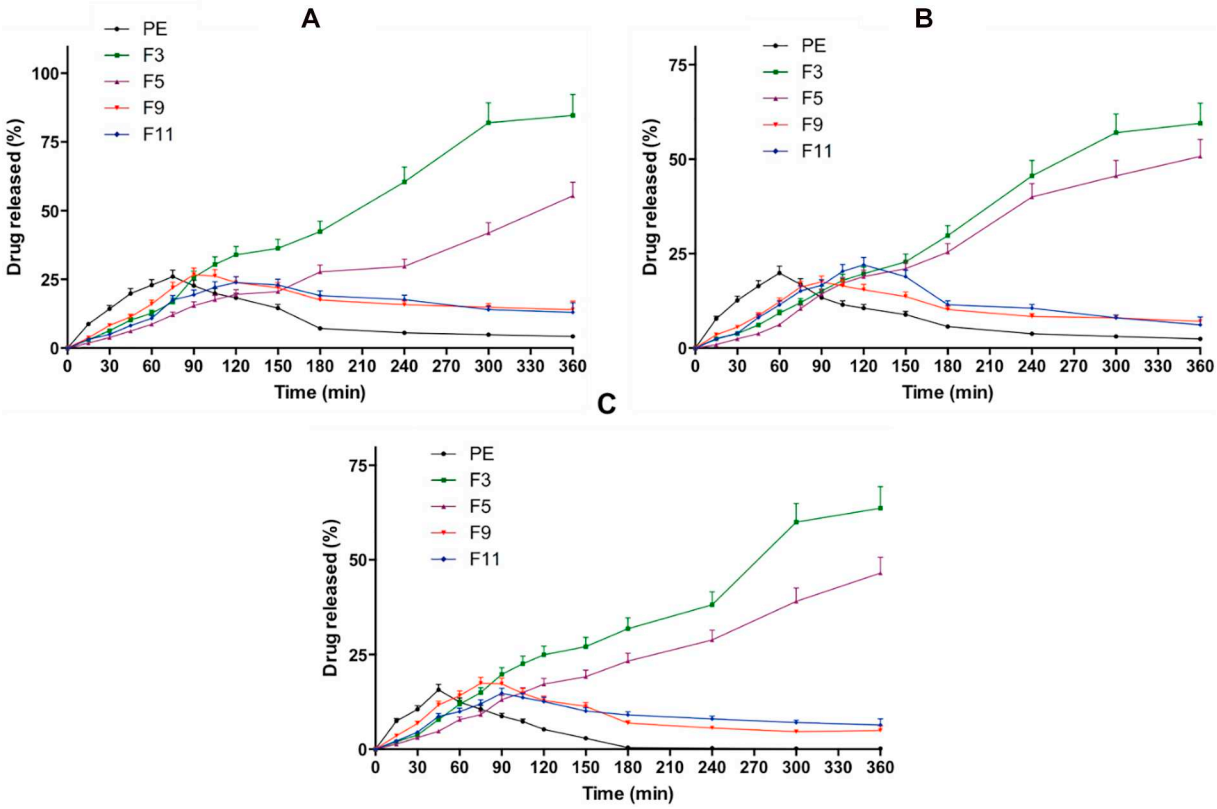

Fig. 5. *In vitro* dissolution profiles of CA (A), QU (B) and KP (C) in PE in comparison with different PEP formulations in FaSSIF, pH 6.5 at 37 °C (means ± SD, n = 3).

68.43 ± 6.15% of CA, QU and KP was released from F3 in FaSSIF. In FeSSIF, the total dissolution of 93.89 ± 8.45% of CA, 66.65 ± 6.01% of QU and 69.82 ± 6.28% of KP were dissolved after 6-h from F3. In terms of dissolution behaviour from F5, 59.61 ± 4.98% of CA, 54.54 ± 3.89% of QU and 50.03 ± 4.87% of KP were dissolved in FaSSIF after 6-h. In FeSSIF, approximately 61.45 ± 5.98%, 57.65 ± 5.21% and 51.47 ± 4.65% of CA, QU and KP were dissolved after 6-h, respectively. Our data was supported by Vu et al., developing phytosome formulation of rutin [22] who found that the formulation of rutin into phytosome was able to avoid the degradation of rutin in the intestinal fluid environment. Interestingly, despite the fact that the PEP was able to avoid the degradation, it was not in the case of F9 and F11. Indeed, F9 and F11 were able to delay the degradation of CA, QU and KP in the intestine environment. However, in this study, as shown in Figs. 4 and 5, the degradation still occurred. Degradation was observed in the case of the small particle size of PEP prepared by sonication. Therefore, it could be postulated that, although the small particle size resulted in higher solubility enhancement, the formulations were not rigid enough to protect CA, QU and KP from degradation from the intestine.

3.9. Drug Release Kinetic Using Mathematical Modelling

In an attempt to examine the dissolution mechanism and kinetic modelling of CA, QU and KP from phytosomes, the percentage of drug dissolution data were fitted to different kinetic models. The most suitable release model was selected according to the value of the coefficient correlation of the model investigated. Table S3, S4 and S5 show the results of kinetic modelling profiles of CA, QU and KP from F3, F5, F9 and F11 in different biorelevant media. The results revealed that the release profiles of all compounds from phytosome formulations were best fitted with Higuchi and Korsmeyer-Peppas models. Additionally, the *n* values were between 0.45 and 0.89. Therefore, the dissolution mechanism of CA, QU and KP from phytosome was expected to be non-Fickian (anomalous diffusion). This model illustrates that the release of compounds from the formulation matrix was based on the diffusion of compounds from the matrix, and erosion as well as degradation of the lipid core [65–67]. Analysed statistically, the percentage of dissolution profiles of all compounds from F3 was significantly higher ($p < .05$) compared to the results from F5. For that reason, F3 was selected for further study.

3.10. In vitro Phytosomal Stability in Gastrointestinal Environment

In an attempt to evaluate the physical stability of phytosome following contact with gastrointestinal tract, the particle size, PDI and zeta potential of F3 were investigated for the hypothesised duration in the gastrointestinal tract *in vivo*. Table 4 summarizes the particle size, PDI and zeta potential of F3 in biorelevant media (FaSSGF, FeSSIF and FaSSIF). The results exhibited that there were no statistically significant differences ($p > .05$) in particle size and PDI of F3 following 3 h and 6 h incubation in biorelevant media compared to the initial measurements of F3. In addition to that, it was found that there were no precipitation and aggregation observed in FaSSGF, FeSSIF and FaSSIF media.

The results presented here reflect that phytosome formulations of F3

Table 4
In vitro phytosomal stability of optimised PEP formulation (F3) in FaSSGF, pH 1.6, FeSSIF, pH 5.0 and FaSSIF, pH 6.5 at 37 °C (means ± SD, n = 3).

Time interval	Particle size (nm)	PDI	Zeta potential (mV)
3 h (FaSSGF)	379.36 ± 28.65	0.253 ± 0.01	−15.62 ± 1.12
6 h (FaSSGF)	381.79 ± 28.12	0.268 ± 0.02	−14.98 ± 1.19
3 h (FeSSIF)	383.32 ± 33.31	0.229 ± 0.02	+20.43 ± 1.43
6 h (FeSSIF)	379.99 ± 28.32	0.283 ± 0.02	+21.11 ± 1.32
3 h (FaSSIF)	388.76 ± 24.91	0.212 ± 0.02	+22.23 ± 1.65
6 h (FaSSIF)	382.03 ± 21.32	0.277 ± 0.02	+21.03 ± 1.76

could potentially sustain their original physical properties and homogenous dispersion stability post-incubation in different biorelevant media, indicating excellent physical stability. Examination of the results showed that phytosome possessed a positive zeta potential in acidic FaSSGF medium (˜20 mV) and a lower negative zeta potential in FaSSIF and FeSSIF (˜ −15 mV). These shifts in the vesicular zeta potential might be described due to the double charge of PC used in this study, namely negative charge from phosphate group and positive charge from choline molecule [30]. Acidic FaSSGF medium is deemed to neutralize the negativity of phosphate oxygen leading to the predomination of a positive charge. In contrast, a slightly higher pH of FaSSIF and FeSSIF is deemed to neutralize positive charge of choline, resulting in negative charge of phytosome vesicles. Lower negative value of FaSSIF and FeSSIF in comparison with the initial zeta potential of phytosome in water may be caused by the common ion effect of the PO_4 group on PC, resulting in the suppression of negative charge. However, this low zeta potential value was able to maintain initial physical stability of the phytosome during the time required in the gastrointestinal tract without showing any particle aggregation and precipitation. In addition, the zeta potential analysis results imply that the phytosome does not need relative high repulsion forces for stabilisation because of trivial need for the liquid state on shelf [68].

3.11. Characterisation of Phytosomal Hydrogel

3.11.1. Drug Uniformity Content and pH

Uniformity content assay of three main compounds of PE in the formulation was carried out to evaluate the effect of the formulation process on the distribution of compounds in the final products. The results exhibited that the recoveries of analytes were found to be between 98.43 ± 1.43% and 99.03 ± 1.87% for CA, 97.98 ± 1.76% and 100.32 ± 2.09% for QU and 98.67 ± 1.32 and 99.98 ± 2.01% for KP. This implies that the formulation process did not affect the recovery and homogeneity of all compounds in the hydrogel. In terms of pH of the formulation, the pH of blank hydrogel was found to be 6.54 ± 0.05. Moreover, the pH of PEP-loaded hydrogel was in the range of 5.19 ± 0.04–5.32 ± 0.03. The final pH of the formulations was in the range of skin pH which is 5 to 6 [69], indicating the tolerability of the formulation to the skin.

3.11.2. Spreadability

Spreadability is one of the essential characteristics of hydrogel formulation related to customer compliance. Administration of hydrogels to the skin is more comfortable for patients if the gel exhibits sufficient spreadability [19,43]. Fig. 6A shows the spreadability of control formulation in comparison with the PEP-loaded hydrogel. The results showed that the incorporation PEP into hydrogel formulation did not change ($p > .05$) the spreadability of the final products.

3.11.3. In vitro Skin Occlusivity Evaluation

Skin occlusivity evaluation was carried out *in vitro* to predict the ability of the formulation to maintain the hydration characteristic of the skin [43]. The results of *in vitro* skin occlusivity are exhibited in Fig. 6B. It was found that the incorporation of PEP into hydrogel was able to increase the occlusivity values significantly ($p < .05$). Higher occlusivity could potentially increase the hydration of the skin for 48 h, enabling the drug permeation into deeper layer of the skin due to the reduction of gaps of corneocyte [70]. Analysed statistically, there was no significant ($p > .05$) in occlusivity values between any formulation of PEP-loaded hydrogel.

3.12. Skin Permeation and Retention Studies

Permeation profiles of CA, QU and KP in rat skin after PE-loaded hydrogel administration in comparison with PEP-loaded hydrogel were then investigated. These three compounds are beneficial for the skin because of their capability to prevent skin aging [71–73]. The results exhibited that only 4.65 ± 0.41% of CA, 4.98 ± 0.39% of QU and 5.16 ± 0.32 of KP were able to permeate the skin after the application of PE-loaded hydrogel, indicating poor skin permeation ability of these compounds. In contrast, approximately 4- to 8-fold higher of these compounds permeated through the skin following the administration of PEP-loaded hydrogel. In F3, 32.36 ± 2.98%, 30.65 ± 2.61% and 32.78 ± 2.12% of CA, QU and KP, respectively, were found in the receptor compartments after 24 h study. In F5, a total permeation of 30.62 ± 2.12%, 28.43 ± 1.98% and 30.98 ± 1.22% were found in the receptor compartment after 24 h in the case of CA, QU and KP, respectively. With respect to the total permeation after F9 administration, 34.65 ± 3.21% of CA, 37.11 ± 3.08% of QU and 42.09 ± 3.56% of KP were able to permeate through the skin after 24 h. In F11, 31.87 ± 2.09% of CA, 35.11 ± 3.09% of QU and 39.11 ± 1.98% of KP were determined in the receptor compartments after 24 h study. Analysed statistically, there were no significant differences ($p > .05$) in the percentage of drug permeated between F3 and F5 and between F9 and F11. As shown in Fig. 6C, D and E, the permeation of all three compounds were very low in the case of PE-loaded hydrogel. This is might be due to the poor skin absorption of phenolic compounds in PE, resulting in poor permeation profiles. It has been reported that the active substances in PE possessed poor permeation characteristic in conventional semisolid preparation [20]. Essentially, the incorporation of PE into phytosomes significantly enhanced the permeation of active compounds through the skin. The increase in permeation might be caused by the strong hydrogen bond generated which could potentially increase the skin absorption of compounds [33]. Moreover, PC contained in the PEP held an important role in transporting the phenolic compounds *via* the lipophilic *stratum corneum* to epidermis and dermis area and passing the hydrophilic nature of viable dermis [24].

Skin drug retention is a critical factor affecting the efficacy of anti-aging product. The higher the dermal retention of the formulation, the higher the ability of the antioxidant compound to prevent lipoperoxidation in the skin [11]. As mentioned previously, the nature of CA, QU and KP resulted in low drug retention in the skin. After 24, only 3.56 ± 0.31% of CA, 4.98 ± 0.42% of QU and 6.51 ± 0.54% of KP were retained in the skin (Fig. 6F). Essentially, the drug retention after 24 h following PEP-loaded hydrogel was varying between 12.65 ± 1.01% and 33.09 ± 2.98% in all formulations. The highest retention of drugs was achieved by F5 with 26.78 ± 1.12% of CA, 29.78 ± 2.19% of QU and 33.09 ± 2.91% of KP were retained after 24 h application of F5.

3.13. Antioxidant Activity and Sun Protective Factor (SPF) of Optimised Formulation

The antioxidant activities of F3 and F5 of phytosome were evaluated. The IC_{50} against DPPH was found to be 46.65 ± 4.09 μg/mL and 47.76 ± 4.98 μg/mL for F3 and F5, respectively. The IC_{50} in lipid peroxidation inhibition were 68.43 ± 5.12 μg/mL for F3 and 67.19 ± 6.03 μg/mL. Analysed statistically, there was no significant difference ($p = .0003$) between the IC_{50} of PE before and after the phytosome formulations. Therefore, the formulation process did not affect the antioxidant property of PE. Importantly, SPF values of PE, F3 and F5 formulation were found to be 17. 54 ± 2.09, 16.98 ± 1.88 and 17.03 ± 1.92, respectively. It has been previously reported that the SPF values of 15 of higher is considered as broad spectrum [74]. Additionally, PE, F3 and F5 showed radiation absorption in both UVA and UVB wavelength, indicating the high photoprotective of propolis.

Taken together, the findings presented in this study indicate that the phytosomal formulations of propolis lead to enhancement in both oral and dermal routes of the phenolic bioactive compounds, namely CA, QU and KP. These results have provided a new insight in the development of suitable delivery system for naturally-occurring antioxidant

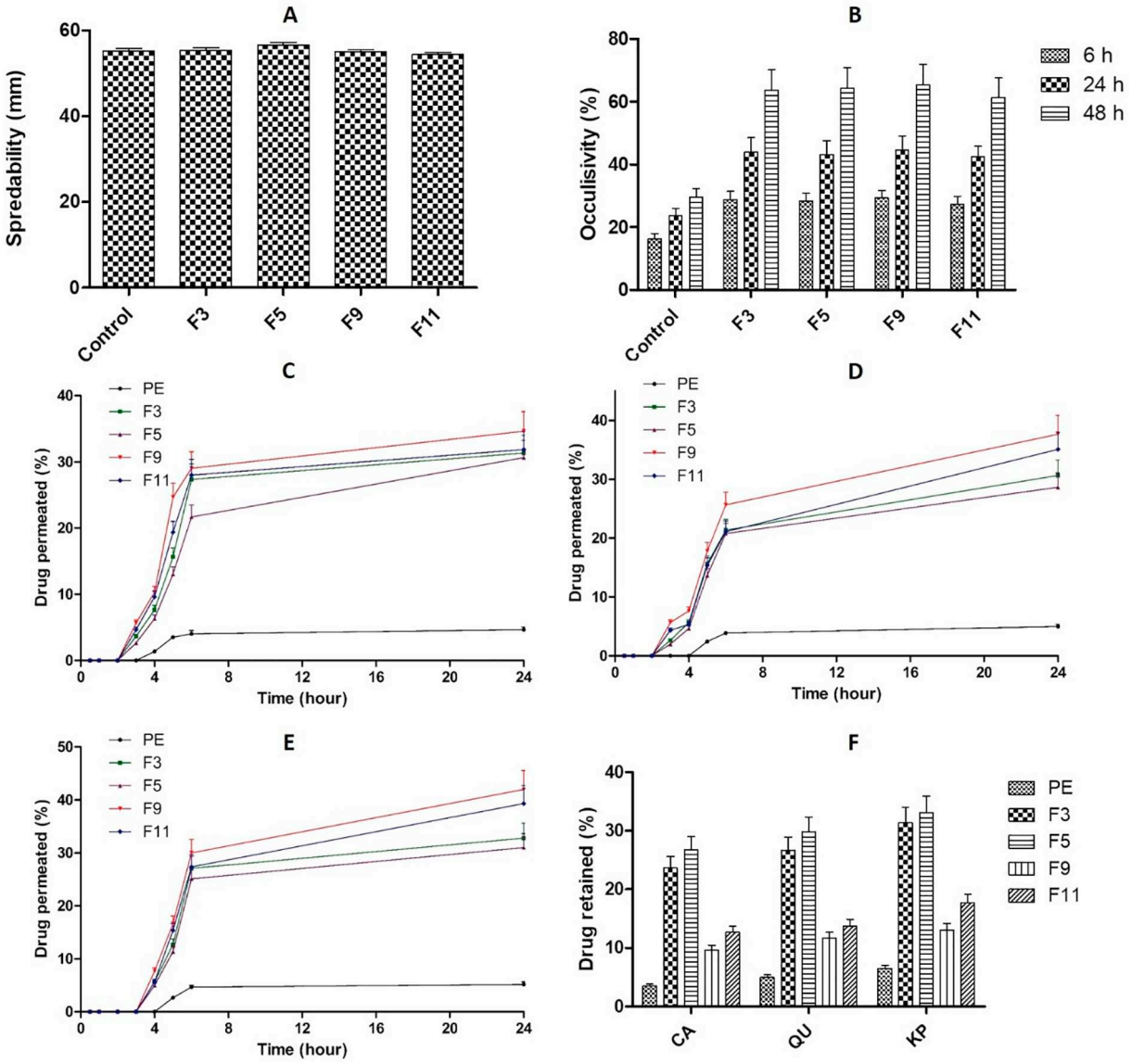

Fig. 6. Spreadability of PEP-loaded hydrogel formulation in comparison with control hydrogel (A), *In vitro* skin occlusivity of PEP-loaded hydrogel formulation in comparison with control hydrogel (B), *in vitro* skin permeation profiles of CA (C), QU (D) and KP (E) in PE in comparison with different PEP formulations and skin drug retention profiles of CA, QU and KP after 24 h permeation study (F) (means ± SD, n = 3).

compounds contained in propolis. Enhanced dissolution profile and better stability were observed in *in vitro* assays for the oral route of administration of PEP. Likewise, for the dermal route, increased penetrability and higher skin retention were showed by the phytosomal formulations. Moving toward, future studies are now warranted to evaluate the long-term stability of this approach. In addition, the *in vivo* pharmacokinetic profiles of the antioxidant compounds of PE following the administration of this innovative approach should also be carried out. Following this, the toxicity and pharmacodinamic studies in an appropriate system should also be carried out.

4. Conclusion

This study investigated the potential of a novel phytosome delivery system to enhance the dissolution profile of three main bioactive compounds from propolis having antioxidative activity, namely CA, QU and KP. Optimum TPC, TFC and antioxidant activity was achieved using 75% *v*/v ethanol as an extraction solvent. Importantly, using this solvent, the concentration of CA, QU and KP were higher compared to those from other solvents. Several optimisations and characterisations were then carried out to develop the PEP formulation. By using thin-film hydration method, and further homogenisation process for 10 min, the optimum spherical PEP was achieved with a particle size, PDI and zeta potential of 364.82 ± 31.74 nm, 0.244 ± 0.02 and − 34.09 ± 2.96 mV for F3, and 473.97 ± 41.24 nm, 0.265 ± 0.02 and − 37.41 ± 3.26 mV for F5, respectively. Essentially, the encapsulations of CA, QU and KP in optimised PEP formulation were more than 40%. FTIR study confirmed the formation of phytosome by the appearance of new hydrogen bonds formed between bioactive compound in PE and PC. Furthermore, compared to unformulated extract, the solubility and dissolution behaviour of CA, QU and KP in three different biorelevant media were significantly enhanced. Additionally, the skin retentions of three compounds were improved using this phytosomal approach. Finally, the physical characteristic of optimised PEP and the antioxidant activity of PE in PEP formulation did not exhibited significant reduction, indicating that the successful approach has been achieved. The utilisation of phytosome delivery system provides proof of principle for the enhanced the stability of and dissolution behaviour of hydrophobic compounds in natural products which could, therefore, increase the bioavailability of

these compounds. In addition, the improved skin retention of these compounds following the administration of PEP demonstrated the high possibility of PE to inhibit the stress oxidative in the skin. Essentially, the optimised hydrogel formulations exhibited broad spectrum for UVA and UVB radiation absorption, with the SPF values of > 15. However, before investigating the effectiveness of this delivery approach, further broad studies are required, including *in vivo* pharmacokinetics, toxicity and pharmacodynamic studies in a suitable model system.

Declaration of Competing Interest

The authors declare no conflict of interest.

Acknowledgements

The authors thank the Ministry of Education, Indonesia for funding this study.

Appendix A. Supplementary data

Supplementary data to this article can be found online at https://doi.org/10.1016/j.jphotobiol.2020.111846.

References

[1] V. Lobo, A. Patil, A. Phatak, N. Chandra, Free radicals, antioxidants and functional foods: impact on human health, Pharmacogn. Rev. 4 (2010) 118–126.
[2] A.H. Bhat, K.B. Dar, S. Anees, M.A. Zargar, A. Masood, M.A. Sofi, S.A. Ganie, Oxidative stress, mitochondrial dysfunction and neurodegenerative diseases; a mechanistic insight, Biomed. Pharmacother. 74 (2015) 101–110.
[3] G. Ndrepepa, Myeloperoxidase – a bridge linking inflammation and oxidative stress with cardiovascular disease, Clin. Chim. Acta 493 (2019) 36–51.
[4] M.J. Smallwood, A. Nissim, A.R. Knight, M. Whiteman, R. Haigh, P.G. Winyard, Oxidative stress in autoimmune rheumatic diseases, Free Radic. Biol. Med. 125 (2018) 3–14.
[5] D. Li, G. Liang, R. Calderone, J.A. Bellanti, Vitiligo and Hashimoto's thyroiditis: autoimmune diseases linked by clinical presentation, biochemical commonality, and autoimmune/oxidative stress-mediated toxicity pathogenesis, Med. Hypotheses 128 (2019) 69–75.
[6] M. Hemmati-Dinarvand, S. Saedi, M. Valilo, A. Kalantary-Charvadeh, M. Alizadeh Sani, R. Kargar, H. Safari, N. Samadi, Oxidative stress and Parkinson's disease: conflict of oxidant-antioxidant systems, Neurosci. Lett. 709 (2019) 134296.
[7] T. Nakanishi, T. Kuragano, M. Nanami, Y. Nagasawa, Y. Hasuike, Misdistribution of iron and oxidative stress in chronic kidney disease, Free Radic. Biol. Med. 133 (2019) 248–253.
[8] B. Khambu, S. Yan, N. Huda, G. Liu, X.-M. Yin, Autophagy in non-alcoholic fatty liver disease and alcoholic liver disease, Liver Res. 2 (2018) 112–119.
[9] Y. Lin, M. Jiang, W. Chen, T. Zhao, Y. Wei, Cancer and ER stress: mutual crosstalk between autophagy, oxidative stress and inflammatory response, Biomed. Pharmacother. 118 (2019) 109249.
[10] F. Trautinger, Mechanisms of photodamage of the skin and its functional consequences for skin ageing, Clin. Exp. Dermatol. 26 (2001) 573–577.
[11] S. Salvioli, M. Bonafè, M. Capri, D. Monti, C. Franceschi, Mitochondria, aging and longevity - a new perspective, FEBS Lett. 492 (2001) 9–13.
[12] I. Zavodnik, V. Buko, O. Lukivskaya, E. Lapshina, T. Ilyich, E. Belonovskaya, S. Kirko, E. Naruta, I. Kuzmitskaya, G. Budryn, D. Zyzelevicz, J. Orach, A. Zakrzeska, L. Kiryukhina, Cranberry (Vaccinium macrocarpon) peel polyphenol-rich extract attenuates rat liver mitochondria impairments in alcoholic steatohepatitis in vivo and after oxidative treatment in vitro, J. Funct. Foods 57 (2019) 83–94.
[13] A.A. Thabet, F.S. Youssef, M. El-Shazly, H.A. El-Beshbishy, A.N.B. Singab, Validation of the antihyperglycaemic and hepatoprotective activity of the flavonoid rich fraction of Brachychiton rupestris using in vivo experimental models and molecular modelling, Food Chem. Toxicol. 114 (2018) 302–310.
[14] J. Kocot, M. Kiełczykowska, D. Luchowska-Kocot, J. Kurzepa, I. Musik, Antioxidant potential of propolis, bee pollen, and royal jelly: possible medical application, Oxidative Med. Cell. Longev. 2018 (2018) 1–29.
[15] T. Ozdal, F.D. Ceylan, N. Eroglu, M. Kaplan, E.O. Olgun, E. Capanoglu, Investigation of antioxidant capacity, bioaccessibility and LC-MS/MS phenolic profile of Turkish propolis, Food Res. Int. 122 (2019) 528–536.
[16] C.M. Spagnol, R.P. Assis, I.L. Brunetti, V.L.B. Isaac, H.R.N. Salgado, M.A. Corrêa, In vitro methods to determine the antioxidant activity of caffeic acid, Spectrochim. Acta A Mol. Biomol. Spectrosc. 219 (2019) 358–366.
[17] R.A. Dar, P.K. Brahman, N. Khurana, J.A. Wagay, Z.A. Lone, M.A. Ganaie, K.S. Pitre, Evaluation of antioxidant activity of crocin, podophyllotoxin and kaempferol by chemical, biochemical and electrochemical assays, Arab. J. Chem. 10 (2017) S1119–S1128.
[18] L. Simon, M. Vincent, S. Le Saux, V. Lapinte, N. Marcotte, M. Morille, C. Dorandeu, J.M. Devoisselle, S. Bégu, Polyoxazolines based mixed micelles as PEG free formulations for an effective quercetin antioxidant topical delivery, Int. J. Pharm. 570 (2019) 118516.
[19] S. Uprit, R. Kumar Sahu, A. Roy, A. Pare, Preparation and characterization of minoxidil loaded nanostructured lipid carrier gel for effective treatment of alopecia, Saudi Pharm. J. 21 (2013) 379–385.
[20] M. Žilius, K. Ramanauskiene, V. Briedis, Release of propolis phenolic acids from semisolid formulations and their penetration into the human skin in vitro, Evid. Based Complement. Alternat. Med. 2013 (2013).
[21] M. Kfoury, C. Geagea, S. Ruellan, H. Greige-Gerges, S. Fourmentin, Effect of cyclodextrin and cosolvent on the solubility and antioxidant activity of caffeic acid, Food Chem. 278 (2019) 163–169.
[22] H.T.H. Vu, S.M. Hook, S.D. Siqueira, A. Müllertz, T. Rades, A. McDowell, Are phytosomes a superior nanodelivery system for the antioxidant rutin? Int. J. Pharm. 548 (2018) 82–91.
[23] D.R. Telange, A.T. Patil, A.M. Pethe, H. Fegade, S. Anand, V.S. Dave, Formulation and characterization of an apigenin-phospholipid phytosome (APLC) for improved solubility, in vivo bioavailability, and antioxidant potential, Eur. J. Pharm. Sci. 108 (2017) 36–49.
[24] M.K. Das, B. Kalita, Design and evaluation of phyto-phospholipid complexes (phytosomes) of Rutin for transdermal application, J. Appl. Pharm. Sci. 4 (2014) 51–57.
[25] M. Lu, Q. Qiu, X. Luo, X. Liu, J. Sun, C. Wang, X. Lin, Y. Deng, Y. Song, Phyto-phospholipid complexes (phytosomes): a novel strategy to improve the bioavailability of active constituents, Asian J. Pharm. Sci. 14 (2019) 265–274.
[26] A. Shakeri, A. Sahebkar, Opinion paper: phytosome: a fatty solution for efficient formulation of phytopharmaceuticals, Recent Pat. Drug Deliv. Formul. 10 (2016) 7–10.
[27] J. Khan, A. Alexander, Ajazuddin, S. Saraf, S. Saraf, Recent advances and future prospects of phyto-phospholipid complexation technique for improving pharmacokinetic profile of plant actives, J. Control. Release 168 (2013) 50–60.
[28] E. Hammam, J. Basahi, I. Ismail, I. Hassan, T. Almeelbi, The role of hydrogen bonding in the fluorescence quenching of 2,6-bis((E)-2-(benzoxazol-2-yl)vinyl) naphthalene (BBVN) in methanol, Spectrochim. Acta A Mol. Biomol. Spectrosc. 173 (2017) 681–686.
[29] J. Zhao, P. Song, Y. Cui, X. Liu, S. Sun, S. Hou, F. Ma, Effects of hydrogen bond on 2-aminopyridine and its derivatives complexes in methanol solvent, Spectrochim. Acta A Mol. Biomol. Spectrosc. 131 (2014) 282–287.
[30] M.S. Freag, Y.S.R. Elnaggar, O.Y. Abdallah, Lyophilized phytosomal nanocarriers as platforms for enhanced diosmin delivery: optimization and ex vivo permeation, Int. J. Nanomedicine 8 (2013) 2385–2397.
[31] R.P. Singh, H.V. Gangadharappa, K. Mruthunjaya, Phytosome complexed with chitosan for gingerol delivery in the treatment of respiratory infection: in vitro and in vivo evaluation, Eur. J. Pharm. Sci. 122 (2018) 214–229.
[32] P. Ju Ho, J. Jun Sung, K. Ki Cheon, H. Jin Tae, Anti-inflammatory effect of Centella asiatica phytosome in a mouse model of phthalic anhydride-induced atopic dermatitis, Phytomedicine 43 (2018) 110–119.
[33] S. Surini, H. Mubarak, D. Ramadon, Cosmetic serum containing grape (*Vitis vinifera* L.) seed extract phytosome: formulation and in vitro penetration study, J. Young Pharm. 10 (2018) (s51–s55).
[34] J. Chlopicka, P. Pasko, S. Gorinstein, A. Jedryas, P. Zagrodzki, Total phenolic and total flavonoid content, antioxidant activity and sensory evaluation of pseudocereal breads, LWT Food Sci. Technol. 46 (2012) 548–555.
[35] K. Thaipong, U. Boonprakob, K. Crosby, L. Cisneros-Zevallos, D. Hawkins Byrne, Comparison of ABTS, DPPH, FRAP, and ORAC assays for estimating antioxidant activity from guava fruit extracts, J. Food Compos. Anal. 19 (2006) 669–675.
[36] A. Meda, C.E. Lamien, M. Romito, J. Millogo, O.G. Nacoulma, Determination of the total phenolic, flavonoid and proline contents in Burkina Fasan honey, as well as their radical scavenging activity, Food Chem. 91 (2005) 571–577.
[37] Q.D. Do, A.E. Angkawijaya, P.L. Tran-Nguyen, L.H. Huynh, F.E. Soetaredjo, S. Ismadji, Y.H. Ju, Effect of extraction solvent on total phenol content, total flavonoid content, and antioxidant activity of Limnophila aromatica, J. Food Drug Anal. 22 (2014) 296–302.
[38] N. Turkmen, F. Sari, Y.S. Velioglu, The effect of cooking methods on total phenolics and antioxidant activity of selected green vegetables, Food Chem. 93 (2005) 713–718.
[39] A.D. Permana, I.A. Tekko, H.O. McCarthy, R.F. Donnelly, New HPLC–MS method for rapid and simultaneous quantification of doxycycline, diethylcarbamazine and albendazole metabolites in rat plasma and organs after concomitant oral administration, J. Pharm. Biomed. Anal. 170 (2019) 243–253.
[40] A.D. Permana, I.A. Tekko, M.T.C. McCrudden, Q.K. Anjani, D. Ramadon, H.O. McCarthy, R.F. Donnelly, Solid lipid nanoparticle-based dissolving microneedles: a promising intradermal lymph targeting drug delivery system with potential for enhanced treatment of lymphatic filariasis, J. Control. Release 316 (2019) 34–52.
[41] A.D. Permana, M.T.C. McCrudden, R.F. Donnelly, Enhanced intradermal delivery of nanosuspensions of antifilariasis drugs using dissolving microneedles: a proof of concept study, Pharmaceutics 11 (2019) 346.
[42] Y. Zhang, M. Huo, J. Zhou, A. Zou, W. Li, C. Yao, S. Xie, DDSolver: an add-in program for modeling and comparison of drug dissolution profiles, AAPS J. 12 (2010) 263–271.
[43] D.S. Malik, G. Kaur, Nanostructured gel for topical delivery of azelaic acid: designing, characterization, and in-vitro evaluation, J. Drug Deliv. Sci. Technol. 47 (2018) 123–136.
[44] J.S. de Mansur, M.N.R. Breder, M.C. d'Ascenção Mansur, R.D. Azulay, Correlação entre a determinaçäo do fator de proteçäo solar em seres humanos e por

espectrofotometria, An. Bras. Dermatol. 61 (1986) 121–124.
[45] S. Kalthoff, C.P. Strassburg, Contribution of human UDP-glucuronosyltransferases to the antioxidant effects of propolis, artichoke and silymarin, Phytomedicine 56 (2019) 35–39.
[46] V. Tzankova, D. Aluani, Y. Yordanov, M. Kondeva-Burdina, P. Petrov, V. Bankova, R. Simeonova, V. Vitcheva, F. Odjakov, A. Apostolov, B. Tzankov, K. Yoncheva, Micellar propolis nanoformulation of high antioxidant and hepatoprotective activity, Brazilian J. Pharmacogn. 29 (2018) 364–372.
[47] B. King-Díaz, J. Granados-Pineda, M. Bah, J.F. Rivero-Cruz, B. Lotina-Hennsen, Mexican propolis flavonoids affect photosynthesis and seedling growth, J. Photochem. Photobiol. B Biol. 151 (2015) 213–220.
[48] C. Sun, Z. Wu, Z. Wang, H. Zhang, Effect of ethanol/water solvents on phenolic profiles and antioxidant properties of Beijing propolis extracts, Evid. Based Complement. Alternat. Med. 2015 (2015) 1–9.
[49] A. Mazumder, A. Dwivedi, J.L. Du Preez, J. Du Plessis, In vitro wound healing and cytotoxic effects of sinigrin-phytosome complex, Int. J. Pharm. 498 (2016) 283–293.
[50] A.I. Abd El-Fattah, M.M. Fathy, Z.Y. Ali, A.E.R.A. El-Garawany, E.K. Mohamed, Enhanced therapeutic benefit of quercetin-loaded phytosome nanoparticles in ovariectomized rats, Chem. Biol. Interact. 271 (2017) 30–38.
[51] Y. Zu, W. Sun, X. Zhao, W. Wang, Y. Li, Y. Ge, Y. Liu, K. Wang, Preparation and characterization of amorphous amphotericin B nanoparticles for oral administration through liquid antisolvent precipitation, Eur. J. Pharm. Sci. 53 (2014) 109–117.
[52] S. Das, W.K. Ng, P. Kanaujia, S. Kim, R.B.H. Tan, Formulation design, preparation and physicochemical characterizations of solid lipid nanoparticles containing a hydrophobic drug: effects of process variables, Colloids Surf. B: Biointerfaces 88 (2011) 483–489.
[53] S.F. El-Menshawe, A.A. Ali, M.A. Rabeh, N.M. Khalil, Nanosized soy phytosome-based thermogel as topical anti-obesity formulation: an approach for acceptable level of evidence of an effective novel herbal weight loss product, Int. J. Nanomedicine 13 (2018) 307–318.
[54] B. Demir, F.B. Barlas, E. Guler, P.Z. Gumus, M. Can, M. Yavuz, H. Coskunol, S. Timur, Gold nanoparticle loaded phytosomal systems: synthesis, characterization and in vitro investigations, RSC Adv. 4 (2014) 34687–34695.
[55] National Center for Biotechnology Information, Quercetin, PubChem Database, 1 (2019) https://pubchem.ncbi.nlm.nih.gov/compound/Quercetin (accessed August 3, 2019).
[56] National Center for Biotechnology Information, Caffeic acid, PubChem Database, 1 (2019) https://pubchem.ncbi.nlm.nih.gov/compound/Caffeic-acid (accessed August 3, 2019).
[57] National Center for Biotechnology Information, Kaempferol, PubChem Database, 1 (2019) https://pubchem.ncbi.nlm.nih.gov/compound/Kaempferol (accessed August 3, 2019).
[58] A.R. Machado, L.M. Assis, J.A.V.V. Costa, E. Badiale-Furlong, A.S. Motta, Y.M.S.S. Micheletto, L.A. Souza-Soares, Application of sonication and mixing for nanoencapsulation of the cyanobacterium Spirulina platensis in liposomes, Int. Food Res. J. 21 (2014) 2201–2206.
[59] F. Kesisoglou, M. Wang, K. Galipeau, P. Harmon, G. Okoh, W. Xu, Effect of amorphous nanoparticle size on bioavailability of anacetrapib in dogs, J. Pharm. Sci. (2019) 1–9.
[60] M. Sharma, R. Sharma, D.K. Jain, A. Saraf, Enhancement of oral bioavailability of poorly water soluble carvedilol by chitosan nanoparticles: optimization and pharmacokinetic study, Int. J. Biol. Macromol. 135 (2019) 246–260.
[61] B. Albertini, S. Bertoni, B. Perissutti, N. Passerini, An investigation into the release behavior of solid lipid microparticles in different simulated gastrointestinal fluids, Colloids Surf. B: Biointerfaces 173 (2019) 276–285.
[62] N. Borkar, D. Xia, R. Holm, Y. Gan, A. Müllertz, M. Yang, H. Mu, Investigating the correlation between in vivo absorption and in vitro release of fenofibrate from lipid matrix particles in biorelevant medium, Eur. J. Pharm. Sci. 51 (2014) 204–210.
[63] F. Jung, L. Nothnagel, F. Gao, M. Thurn, V. Vogel, M.G. Wacker, A comparison of two biorelevant in vitro drug release methods for nanotherapeutics based on advanced physiologically-based pharmacokinetic modelling, Eur. J. Pharm. Biopharm. 127 (2018) 462–470.
[64] C.J. Andreas, Y.C. Chen, C. Markopoulos, C. Reppas, J. Dressman, In vitro biorelevant models for evaluating modified release mesalamine products to forecast the effect of formulation and meal intake on drug release, Eur. J. Pharm. Biopharm. 97 (2015) 39–50.
[65] Y. Gao, J. Zuo, N. Bou-Chacra, T.J.A. de Pinto, S.-D. Clas, R.B. Walker, R. Löbenberg, In vitro release kinetics of antituberculosis drugs from nanoparticles assessed using a modified dissolution apparatus, Biomed. Res. Int. 2013 (2013) 1–9.
[66] P. Costa, J.M.S. Lobo, Modeling and comparison of dissolution profiles, Eur. J. Pharm. Sci. 13 (2001) 123–133.
[67] S. Dash, P.N. Murthy, L. Nath, P. Chowdhury, Kinetic modelling on drug release from controlled drug delivery systems, Acta Pol. Pharm. Drug Res. 67 (2010) 217–223.
[68] M.A. Elsheikh, Y.S.R. Elnaggar, E.Y. Gohar, O.Y. Abdallah, Nanoemulsion liquid preconcentrates for raloxifene hydrochloride: optimization and in vivo appraisal, Int. J. Nanomedicine 7 (2012) 3787–3802.
[69] A. Seweryn, T. Bujak, Application of anionic phosphorus derivatives of alkyl polyglucosides for the production of sustainable and mild body wash cosmetics, ACS Sustain. Chem. Eng. 6 (2018) 17294–17301.
[70] H.O. Ammar, M.M. Ghorab, D.M. Mostafa, E.S. Ibrahim, Folic acid loaded lipid nanocarriers with promoted skin antiaging and antioxidant efficacy, J. Drug Deliv. Sci. Technol. 31 (2016) 72–82.
[71] S. Pientaweeratch, V. Panapisal, A. Tansirikongkol, Antioxidant, anti-collagenase and anti-elastase activities of Phyllanthus emblica, Manilkara zapota and silymarin: an in vitro comparative study for anti-aging applications, Pharm. Biol. 54 (2016) 1865–1872.
[72] C. Magnani, V.L.B. Isaac, M.A. Correa, H.R.N. Salgado, Caffeic acid: a review of its potential use in medications and cosmetics, Anal. Methods 6 (2014) 3203–3210.
[73] T.P. Pivetta, L.B. Silva, C.M. Kawakami, M.M. Araújo, M.P.F.M. Del Lama, R.M.Z.G. Naal, S.S. Maria-Engler, L.R. Gaspar, P.D. Marcato, Topical formulation of quercetin encapsulated in natural lipid nanocarriers: evaluation of biological properties and phototoxic effect, J. Drug Deliv. Sci. Technol. 53 (2019) 101148.
[74] A.R. Nunes, A.L.M. Rodrigues, D.B. de Queiróz, I.G.P. Vieira, J.F.C. Neto, J.T.C. Junior, S.R. Tintino, S.M. de Morais, H.D.M. Coutinho, Photoprotective potential of medicinal plants from Cerrado biome (Brazil) in relation to phenolic content and antioxidant activity, J. Photochem. Photobiol. B Biol. 189 (2018) 119–123.